DOI: 10.1021/ic100591h

Inorganic Chemistry
Article

Manganese(II)-Octacyanometallate(V) Bimetallic Ferrimagnets with T_c from 41 to 53 K Obtained in Acidic Media[⊥]

Tian-Wei Wang,[†] Jun Wang,[†] Shin-ichi Ohkoshi,[‡] You Song,*[,†] and Xiao-Zeng You*[,†]

[†]*State Key Laboratory of Coordination Chemistry, Nanjing National Laboratory of Microstructures School of Chemistry and Chemical Engineering, Nanjing University, Nanjing, China, 210093, and* [‡]*Department of Chemistry, School of Science, The University of Tokyo, 7-3-1 Hongo, Bunkyo-ku, Toyko 113-0033, Japan*

Received March 29, 2010

A series of three-dimensional (3D) octacyanometallate-based bimetallic magnets, $\{[Mn(H_2O)][Mn_{0.75}(HCOO)_{0.5}(H_2O)_{0.5}][W(CN)_8]\cdot H_2O\}_{4n}$ (**1**), $\{[Mn_2(HCOO)(HCOOH)][M(CN)_8]\cdot H_2O\}_n$ (M = W (**2**) and Mo (**3**)), and $\{[Mn_2(HCOO)(HCOOH)][W(CN)_8]\cdot CH_3OH\}_n$ (M = W (**4**) and Mo (**5**)), were synthesized by the reaction of octacyanometallates $A_3[M(CN)_8]\cdot nH_2O$ (A = Na, Cs, and $(C_4H_9)_3NH$; M = W and Mo; and n = 2 or 4) with manganese salt ($Mn(CH_3COO)_2\cdot 4H_2O$, $Mn(ClO_4)_2\cdot 6H_2O$, and $MnCl_2\cdot 4H_2O$) in aqueous or methanolic solution containing formic acid. All complexes crystallize in the tetragonal or orthorhombic system. Complex **1** shows an unexpected 3D network structure by connections of manganese ions and octacyanotangstate−manganese double layers via cyanide bridges, while other complexes have typical structure constructions similar to the reported complexes $\{[MnL]_m[M(CN)_8]\}_n$ (L = CH_3COO^-, Cl^-, and H_2O), which the CN group of $[W^V(CN)_8]$ coordinates to eight Mn^{II} ions forming a $-[W(CN)_8]-Mn_4-[W(CN)_8]-Mn_4-$ columnar chain, and then all chains share Mn^{II} ions as the nodes interlocking with each other to form the 3D networks. Magnetic studies indicate that the cyanide group mediates the antiferromagnetic coupling between octacyanometallates and manganese ions in all complexes, and the ferrimagnetic phase transition temperatures are 53, 52, 42, 49, and 41 K for **1**−**5**, respectively.

Introduction

In the past decades the molecular magnets of Prussian blue and its analogs have attracted special attention in the field of material science because the cyanide can effectively mediate magnetic coupling between metal ions, leading to the three-dimensional (3D) magnets with a high critical temperature (T_c).[1] As a building block, octacyanometallates $[M(CN)_8]^{n-}$ (M = Mo, W, and Nb) are good candidates for mediating the magnetic exchange interaction because of their unique features, such as multicoordination number, versatile configurations, and more diffused 4d and 5d orbitals.[2−6] All of these merits make octacyanometallate-based magnets have a relatively high T_c, thereby octacyanometallate is a promising building block for molecular magnets.

The metal center ions in octacyanometallates are with two valence states of +4 and +5. An alkali or neutral solution always stabilizes the diamagnetic +4 state,[6g,7] so acidic media is usually used for synthesizing octacyanometallate-based

[⊥] This work is dedicated to the memory of Prof. Robert Bau (1944−2008).

*To whom correspondence should be addressed. E-mail: yousong@nju.edu.cn (Y.S.), youxz@nju.edu.cn (X.-Z.Y.).

(1) Typical examples: (a) Mallah, T.; Thiébaut, S.; Verdaguer, M.; Veillet, P. *Science* **1993**, *262*, 1554. (b) Entley, W. R.; Girolami, G. S. *Science* **1995**, *268*, 397. (c) Ferlay, S.; Mallah, T.; Ouahès, R.; Veillet, P.; Verdaguer, M. *Nature* **1995**, *378*, 701. (d) Sato, O.; Iyoda, T.; Fujishima, A.; Hashimoto, K. *Science* **1996**, *271*, 49. (e) Dujardin, E.; Ferlay, S.; Phan, X.; Desplanches, C.; Cartier dit Moulin, C.; Sainctavit, P.; Baudelet, F.; Dartyge, E.; Veillet, P.; Verdaguer, M. *J. Am. Chem. Soc.* **1998**, *120*, 11347. (f) Holmes, S. M.; Girolami, G. S. *J. Am. Chem. Soc.* **1999**, *121*, 5593. (g) Verdaguer, M.; Bleuzen, A.; Marvaud, V.; Vaissermann, J.; Seuleiman, M.; Desplanches, C.; Scuiller, A.; Train, C.; Garde, R.; Gelly, G.; Lomenech, C.; Rosenman, I.; Veillet, P.; Cartier, C.; Villain, F. *Coord. Chem. Rev.* **1999**, *190*−*192*, 1023.

(2) (a) Sieklucka, B.; Podgajny, R.; Przychodzeń, P.; Korzeniak, T. *Coord. Chem. Rev.* **2005**, *249*, 2203, and references therein. (b) Przychodzeń, P.; Korzeniak, T.; Podgajny, R.; Sieklucka, B. *Coord. Chem. Rev.* **2006**, *250*, 2234, and references therein. (c) Sieklucka, B.; Podgajny, R.; Pinkowicz, D.; Nowicka, B.; Korzeniak, T.; Baanda, M.; Wasiutyński, T.; Peka, R.; Makarewicz, M.; Czapla, M.; Rams, M.; Gawe, B.; Łasocha, W. *CrystEngComm* **2009**, *11*, 2032, and references therein. (d) Sieklucka, B.; Podgajny, R.; Korzeniak, T.; Przychodzeń, P.; Kania, R. *C. R. Chim.* **2002**, 639.

(3) Zero-dimensional: (a) Zhong, Z. J.; Seino, H.; Mizobe, Y.; Hidai, M.; Fujishima, A.; Ohkoshi, S.; Hashimoto, K. *J. Am. Chem. Soc.* **2000**, *122*, 2952. (b) Larionova, J.; Gross, M.; Pilkington, M.; Andres, H.; Stoeckli-Evans, H.; Güdel, H. U.; Decurtins, S. *Angew. Chem., Int. Ed.* **2000**, *39*, 1605. (c) Pradhan, R.; Desplanches, C.; Guionneau, P.; Sutter, J.-P. *Inorg. Chem.* **2003**, *42*, 6607. (d) Song, Y.; Zhang, P.; Ren, X.-M.; Shen, X.-F.; Li, Y.-Z.; You, X.-Z. *J. Am. Chem. Soc.* **2005**, *127*, 3708. (e) Freedman, D. E.; Bennett, M. V.; Long, J. R. *Dalton Trans.* **2006**, 2829. (f) Lim, J. H.; Yoon, J. H.; Kim, H. C.; Hong, C. S. *Angew. Chem., Int. Ed.* **2006**, *45*, 7424. (g) Venkatakrishnan, T. S.; Rajamani, R.; Ramasesha, S.; Sutter, J.-P. *Inorg. Chem.* **2007**, *46*, 9569. (h) Hilfiger, M. G.; Zhao, H.; Prosvirin, A.; Wernsdorfer, W.; Dunbar, K. R. *Dalton Trans.* **2009**, 5155. (i) Sutter, J.-P.; Dhers, S.; Rajamani, R.; Ramasesha, S.; Costes, J.-P.; Duhayon, C.; Vendier, L. *Inorg. Chem.* **2009**, *48*, 5820. (j) Wang, J.; Zhang, Z.-C.; Wang, H.-S.; Kang, L.-C.; Zhou, H.-B.; Song, Y.; You, X.-Z. *Inorg. Chem.* **2010**, *49*, 3101. (k) Wang, J.; Xu, Y.-L.; Zhou, H.-B.; Wang, H.-S.; Song, X.-J.; Song, Y.; You, X.-Z. *Dolton Trans.* **2010**, 3489. (l) Ma, S. L.; Ren, S.; Ma, Y.; Liao, D. Z.; Yan, S. P. *Struct. Chem.* **2009**, *20*, 161. (m) Podgajny, R.; Desplanches, C.; Sieklucka, B.; Sessoli, R.; Villar, V.; Paulsen, C.; Wernsdorfer, W.; Dromzée, D.; Verdaguer, M. *Inorg. Chem.* **2002**, *41*, 1323.

Published on Web 08/02/2010

molecular magnets. In our previous work, we prepared manganese(II)−octacyanotungstate(V) magnets by introducing the competition between H^+ and acetic anions in the formation process of the complex.[6b] In the process, acetic anions coordinate to manganese(II) ions with cyanide groups not only for the charge balance but also for modulating the coordination microenvironments and mediating magnetic coupling between Mn^{II} ions. Thus, it is believed that the variation in the accessorial ligand will result in new complex species and will even improve the magnetic properties. According to this strategy, when formic acid was used instead of acetic acid as the acidic media, a series of octacyanometallate-based bimetallic magnets, $\{[Mn(H_2O)][Mn_{0.75}(HCOO)_{0.5}(H_2O)_{0.5}][W(CN)_8]\cdot H_2O\}_{4n}$ (**1**), $\{[Mn_2(HCOO)(HCOOH)][M(CN)_8]\cdot H_2O\}_n$ (M = W (**2**) and Mo (**3**)), and $\{[Mn_2(HCOO)(HCOOH)][M(CN)_8]\cdot CH_3OH\}_n$ (M = W (**4**) and Mo (**5**)), were obtained by reaction of octacyanometallates, $A_3[M(CN)_8]\cdot nH_2O$ (A = Na, Cs, and $(C_4H_9)_3NH$; M = W and Mo; and n = 2 or 4), with manganese salt ($Mn(CH_3COO)_2\cdot 4H_2O$, $Mn(ClO_4)_2\cdot 6H_2O$ and $MnCl_2\cdot 4H_2O$) in an aqueous or methanolic solution. Herein, we report the synthesis, single crystal structures and magnetic properties of octacyanometallate-based bimetallic magnets.

Experimental Section

Materials. The precursors $Cs_3[W(CN)_8]\cdot 2H_2O$, $Na_3[Mo(CN)_8]\cdot 2H_2O$, $(Bu_3NH)_3[W(CN)_8]\cdot 4H_2O$, and $(Bu_3NH)_3[Mo(CN)_8]\cdot 4H_2O$ were prepared according to literature methods.[8,9] All other chemicals were purchased from commercial sources and used without further purification.

Caution! *Cyanides are hyper-toxic and hazardous, and perchlorate salts are potentially explosive. So handing them carefully with small quantities is highly suggested, and all corresponding operations should be done in a fume hood for safety consideration.*

Preparation of $\{[Mn(H_2O)][Mn_{0.75}(HCOO)_{0.5}(H_2O)_{0.5}][W(CN)_8]\cdot H_2O\}_{4n}$ (1). The single crystals of complex **1** suitable for X-ray crystallography were grown by diffusion in a test tube. The manganese(II) acetate tetrahydrate solid (100 mg, ∼0.4 mmol) was put in the bottom of a test tube, and 9 mL of formic acid was added carefully along the tube wall as the bottom layer. Subsequently, 5 mL of formic acid aqueous solution (V(HCOOH): $V(H_2O)$ = 3:2) as the inter layer and 3 mL of aqueous solution of cesium octacyanotungstate(V) dihydrate (171 mg, ∼0.2 mmol) as the top layer were added also with great care. The test tube was left in dark for four weeks. The dark-red block crystals of **1** were obtained with a yield of 75%. IR: $\nu_{C\equiv N}$ = 2174, 2128 cm^{-1}, and $\nu_{C=O}$ = 1593 cm^{-1}. Elemental analysis (%) calcd for $C_{8.50}H_{5.50}Mn_{1.75}N_8O_{3.50}W$ (**1**): C, 18.37; N, 20.17; H, 1.00. Found: C, 18.70; N, 19.86; H, 1.01.

Preparation of $\{[Mn_2(HCOO)(HCOOH)][W(CN)_8]\cdot H_2O\}_n$ (2), $\{[Mn_2(HCOO)(HCOOH)][Mo(CN)_8]\cdot H_2O\}_n$ (3), $\{[Mn_2(HCOO)(HCOOH)][W(CN)_8]\cdot CH_3OH\}_n$ (4), and $\{[Mn_2(HCOO)(HCOOH)][Mo(CN)_8]\cdot CH_3OH\}_n$ (5). The complexes **2**−**5** were synthesized using a similar procedure to that of complex **1**. All the materials and the amount (mole for solid and volume for liquid) used were the same except that of the manganese salt, octacyanometallate, and solvent, otherwise specified in Table 1. For complex **2**, IR: $\nu_{C\equiv N}$ = 2177, 2132 cm^{-1}, and $\nu_{C=O}$ = 1594 cm^{-1}. Elemental analysis (%) calcd for $C_{10}H_4Mn_2N_8O_5W$: C, 19.66; N, 18.34; H, 0.82. Found: C, 19.78; N, 18.14; H, 0.76. For complex **3**, IR: $\nu_{C\equiv N}$ = 2174, 2134 cm^{-1}, and $\nu_{C=O}$ = 1590 cm^{-1}. Elemental analysis (%) calcd for $C_{10}H_4Mn_2MoN_8O_5$: C, 22.96; N, 21.42; H, 0.96. Found: C, 23.19; N, 21.17; H, 0.72. For complex **4**, IR: $\nu_{C\equiv N}$ = 2174, 2134 cm^{-1}, and $\nu_{C=O}$ = 1612 cm^{-1}. Elemental analysis (%) calcd for $C_{11}H_6Mn_2WN_8O_5$: C, 24.60; N, 20.87; H, 1.31. Found: C, 21.10; N, 18.10; H, 0.89. For complex **5**, IR: $\nu_{C\equiv N}$ = 2174, 2134 cm^{-1}, and $\nu_{C=O}$ = 1597 cm^{-1}. Elemental analysis (%) calcd for $C_{11}H_6Mn_2MoN_8O_5$: C, 24.65; N, 20.90; H, 1.13 Found: C, 23.74; N, 20.21; H, 0.279.

X-ray Data Collections and Structure Determinations. All measurements were made on a Bruker Smart CCD. The data reduction was made with the Bruker SAINT package. Absorption correction was performed using the SADABS program. The structures were solved by direct methods and refined on F^2 by full-matrix least-squares using SHELXL-2000 with anisotropic displacement parameters for all non-hydrogen atoms. The hydrogen atoms were generated geometrically. All computations were carried out using the SHELXTL-2000 program package.[10] Crystal data and details of data collections and refinements for **1**−**5** are summarized in Table 2. The selected

(4) One-dimensional: (a) Li, D.-f.; Gao, S.; Zheng, L.-m.; Tang, W.-x. *J. Chem. Soc., Dalton Trans.* **2002**, 2805. (b) Li, D.-F.; Zheng, L.-M.; Zhang, Y.-Z.; Huang, J.; Gao, S.; Tang, W.-X. *Inorg. Chem.* **2003**, *42*, 6123. (c) Przychodzeń, P.; Lewiński, K.; Baanda, M.; Peka, R.; Rams, M.; Wasiutyński, T.; Guyard-Duhayon, C.; Sieklucka, B. *Inorg. Chem.* **2004**, *43*, 2967. (d) You, Y. S.; Kim, D.; Do, Y.; Oh, S. J.; Hong, C. S. *Inorg. Chem.* **2004**, *43*, 6899. (e) Ikeda, S.; Hozumi, T.; Hashimoto, K.; Ohkoshi, S. *Dalton Trans.* **2005**, 2120. (f) Przychodzeń, P.; Lewiński, K.; Peka, R.; Baanda, M.; Tomalac, K.; Sieklucka, B. *Dalton Trans.* **2006**, 625. (g) Przychodzeń, P.; Peka, R.; Lewiński, K.; Supel, J.; Rams, M.; Tomala, K.; Sieklucka, B. *Inorg. Chem.* **2007**, *46*, 8924. (h) Zhao, H.; Shatruk, M.; Prosvirin, A. V.; Dunbar, K. R. *Chem.—Eur. J.* **2007**, *13*, 6573. (i) Prins, F.; Pasca, E.; Jongh, L. J.; Kooijman, H.; Spek, A. L.; Tanase, S. *Angew. Chem., Int. Ed.* **2007**, *46*, 6081. (j) Ma, S.-L.; Ma, Y.; Ren, S.; Yan, S.-P.; Liao, D.-Z. *Struct. Chem.* **2008**, *19*, 329. (k) Zhang, W.; Wang, Z.-Q.; Sato, O.; Xiong, R.-G. *Cryst. Growth Des.* **2009**, *9*, 2050. (k) Choi, S. W.; Ryu, D. W.; Lee, J. W.; Yoon, J. H.; Kim, H. C.; Lee, H.; Cho, B. K.; Hong, C. S. *Inorg. Chem.* **2009**, *48*, 9066. (l) Yoo, H. S.; Ko, H. H.; Ryu, D. W.; Lee, J. W.; Yoon, J. H.; Lee, W. R.; Kim, H. C.; Koh, E. K.; Hong, C. S. *Inorg. Chem.* **2009**, *48*, 5617.

(5) Two-dimensional: (a) Podgajny, R.; Korzeniak, T.; Balanda, M.; Wasiutynski, T.; Errington, W.; Kemp, T. J.; Alcock, N. W.; Sieklucka, B. *Chem. Commun.* **2002**, 1138. (b) Ohkoshi, S.; Arimoto, Y.; Hozumi, T.; Seino, H.; Mizobec, Y.; Hashimoto, K. *Chem. Commun.* **2003**, 2772. (c) Hozumi, T.; Ohkoshi, S.; Arimoto, Y.; Seino, H.; Mizobe, Y.; Hashimoto, K. *J. Phys. Chem. B* **2003**, *107*, 11572. (d) Arimoto, Y.; Ohkoshi, S.; Zhong, Z. J.; Seino, H.; Mizobe, Y.; Hashimoto, K. *J. Am. Chem. Soc.* **2003**, *125*, 9240. (e) Korzeniak, T.; Stadnicka, K.; Rams, M.; Sieklucka, B. *Inorg. Chem.* **2004**, *43*, 4811. (f) Kou, H.-Z.; Ni, Z.-H.; Zhou, B. C.; Wang, R.-J. *Inorg. Chem. Commun.* **2004**, *7*, 1150. (g) Korzeniak, T.; Stadnicka, K.; Peka, R.; Baanda, M.; Tomala, K.; Kowalskid, K.; Sieklucka, B. *Chem. Commun.* **2005**, 2939. (h) Withers, J. R.; Li, D.; Triplet, J.; Ruschman, C.; Parkin, S.; Wang, G.; Yee, G. T.; Holmes, S. M. *Inorg. Chem.* **2006**, *45*, 4307. (i) Podgajny, R.; Baanda, M.; Sikora, M.; Borowiec, M.; Spaek, L.; Kapustac, C.; Sieklucka, B. *Dalton Trans.* **2006**, 2801. (j) Ma, S. L.; Ren, S.; Ma, Y.; Liao, D. Z.; Yan, S. P. *Struct. Chem.* **2009**, *20*, 145.

(6) Three-dimensional: (a) Zhong, Z. J.; Seino, H.; Mizobe, Y.; Hidai, M.; Verdaguer, M.; Ohkoshi, S.; Hashimoto, K. *Inorg. Chem.* **2000**, *39*, 5095. (b) Song, Y.; Ohkoshi, S.; Arimoto, Y.; Seino, H.; Mizobe, Y.; Hashimoto, K. *Inorg. Chem.* **2003**, *42*, 1848. (c) Li, D.-f.; Zheng, L.-m.; Wang, X.-y.; Huang, J.; Gao, S.; Tang, W.-x. *Chem. Mater.* **2003**, *15*, 2094. (d) Herrera, J. M.; Bleuzen, A.; Dromzée, Y.; Julve, M.; Lloret, F.; Verdaguer, M. *Inorg. Chem.* **2004**, *42*, 7052. (e) Kashiwagi, T.; Ohkoshi, S.; Seino, H.; Mizobe, Y.; Hashimoto, K. *J. Am. Chem. Soc.* **2004**, *126*, 5024. (f) Tanase, S.; Prins, F.; Smitsb, J. M. M.; Gelder, R. *CrystEngComm.* **2006**, *8*, 863. (g) Wang, Z. -X.; Shen, X.-F.; Wang, J.; Zhang, P.; Li, Y.-Z.; Nfor, E. N.; Song, Y.; Ohkoshi, S.; Hashimoto, K.; You, X.-Z. *Angew. Chem., Int. Ed.* **2006**, *45*, 3287. (h) Ohkoshi, S.; Tsunobuchi, Y.; Takahashi, H.; Hozumi, T.; Shiro, M.; Hashimoto, K. *J. Am. Chem. Soc.* **2007**, *129*, 3084. (i) Ma, S.-L.; Ma, Y.; Ren, S.; Yan, S.-P.; Cheng, P.; Wang, Q.-L.; Liao, D.-Z. *Cryst. Growth Des.* **2008**, *8*, 3761. (j) Wang, Z.-X.; Li, X.-L.; Liu, B.-L.; Tokoro, H.; Zhang, P.; Song, Y.; Ohkoshi, S.; Hashimoto, K.; You, X.-Z. *Dalton Trans.* **2008**, 2103. (k) Pinkowicz, D.; Podgajny, R.; Baanda, M.; Makarewicz, M.; Gawe, B.; Łasocha, W.; Sieklucka, B. *Inorg. Chem.* **2008**, *47*, 9745. (l) Podgajny, R.; Nitek, W.; Rams, M.; Sieklucka, B. *Cryts. Growth Des.* **2008**, *8*, 3817. (m) Ma, S. L.; Ren, S.; Ma, Y.; Liao, D. Z.; Yan, S. P. *Struct. Chem.* **2009**, *20*, 145.

(7) (a) Wang, Z.-X.; Zhang, P.; Shen, X.-F.; Song, Y.; You, X.-Z.; Hashimoto, K. *Cryts. Growth Des.* **2006**, *6*, 2457. (b) Wang, Z.-X.; Wei, J.; Li, Y.-Z.; Guo, J.-S.; Song, Y. *J. Mol. Struct.* **2008**, *875*, 198.

(8) Leipoldt, J. D.; Bok, L. D. C.; Chilliers, P. J. *Z. Anorg. Allg. Chem.* **1974**, *407*, 350.

(9) Bok, L. D. C.; Leipoldt, J. D.; Basson, S. S. *Z. Anorg. Allg. Chem.* **1975**, *415*, 81.

(10) *SMART, SAINT, SADABS, and SHELXTL*; Bruker AXS Inc.: Madison, WI, 2000.

Table 1. Synthesis of Complexes **1**−**5**

reactants		solvent	products	yield based on Mo or W ions (%)
$Mn(CH_3COO)_2\cdot 4H_2O$	$Cs_3[W(CN)_8]\cdot 2H_2O$	H_2O	**1**	75
$Mn(ClO4)_2\cdot 6H_2O$	$Cs_3[W(CN)_8]\cdot 2H_2O$	H_2O	**2**	36
$MnCl_2\cdot 4H_2O$	$Cs_3[W(CN)_8]\cdot 2H_2O$	H_2O	**2**	24
$Mn(ClO4)_2\cdot 6H_2O$	$Na_3[Mo(CN)_8]\cdot 2H_2O$	H_2O	**3**	26
$MnCl_2\cdot 4H_2O$	$Na_3[Mo(CN)_8]\cdot 2H_2O$	H_2O	**3**	22
$MnCl_2\cdot 4H_2O$	$(NHBu_3)_3[W(CN)_8]\cdot 4H_2O$	CH_3OH	**4**	22
$Mn(ClO4)_2\cdot 6H_2O$	$(NHBu_3)_3[W(CN)_8]\cdot 4H_2O$	CH_3OH	**4**	20
$MnCl_2\cdot 4H_2O$	$(NHBu_3)_3[Mo(CN)_8]\cdot 4H_2O$	CH_3OH	**5**	21
$Mn(ClO4)_2\cdot 6H_2O$	$(NHBu_3)_3[Mo(CN)_8]\cdot 4H_2O$	CH_3OH	**5**	23

Table 2. Crystal Data and Structural Refinement Parameters for Complexes **1**−**5**

	1	**2**	**3**	**4**	**5**
chemical formula	$C_{34}H_{22}Mn_7N_{32}O_4W_4$	$C_{10}H_5Mn_2N_8O_5W$	$C_{10}H_5Mn_2MoN_8O_5$	$C_{11}H_7Mn_2N_8O_5W$	$C_{11}H_7Mn_2MoN_8O_5$
FW (g mol^{-1})	2222.82	610.95	523.04	624.98	537.07
crystal system	tetragonal	orthorhombic	orthorhombic	orthorhombic	orthorhombic
space group	*I*4/*mmm*	*Ibam*	*Ibam*	*Ibam*	*Ibam*
a (Å)	7.6047(6)	10.414(5)	10.419(2)	10.541(3)	10.443(3)
b (Å)	7.6047(6)	12.859(11)	12.837(12)	12.8591(17)	12.854(3)
c (Å)	28.901(4)	13.373(6)	13.371(5)	13.446(2)	13.443(4)
V (Å^3)	1671.4(3)	1790.8(19)	1788.5(18)	1822.6(6)	1804.4(8)
Z	1	4	4	4	4
D (g cm^{-3})	2.208	2.266	1.940	2.278	1.977
reflections (total/unique)	1614/651	4789/923	4510/921	4720/938	4665/931
R/*wR*	0.0321/0.0817	0.0290/0.0764	0.0556/0.1357	0.0370/0.1112	0.0545/0.1328
GOF	1.004	1.088	1.060	1.079	1.073
ρ_{max}/ρ_{min} (e Å^{-3})	0.936/−0.838	0.626/−0.756	0.789/−0.639	1.218/−0.822	0.778/−0.712

Table 3. Selected Bond Lengths (Å) and Angles (°) for **2**−**5**

	2	**3**	**4**	**5**
M1−C1[a]	2.138(5)	2.167(7)	2.176(7)	2.152(6)
M1−C2	2.169(5)	2.155(6)	2.170(7)	2.160(6)
C1−N1	1.150(7)	1.138(8)	1.137(9)	1.146(7)
C2−N2	1.148(6)	1.150(8)	1.165(9)	1.152(7)
N1−Mn1	2.242(4)	2.227(5)	2.224(6)	2.233(5)
N2F−Mn1	2.186(4)	2.191(5)	2.188(6)	2.198(5)
C3−O1	1.270(9)	1.222(10)	1.208(12)	1.222(10)
C3−O2	1.294(8)	1.308(9)	1.312(11)	1.337(10)
M1···C1−N1···Mn1	5.388	5.387	5.413	5.398
M1···C2B−N2B···Mn1A	5.470	5.470	5.495	5.481
M1−C1−N1	178.7(4)	176.8(5)	175.9(5)	176.5(5)
M1−C2−N2	177.7(4)	177.7(5)	177.0(5)	179.0(5)
C1−N1−Mn1	154.1(4)	155.0(5)	158.0(5)	156.7(4)
C2F−N2F−Mn1	168.4(4)	170.1(5)	170.3(5)	168.5(5)

[a] M1 = W1 for **2** and **4** and Mo1 for **3** and **5**. Symmetry codes of A, B, and F are shown in Figure 2.

bond lengths and angles of **1**−**5** are listed in Table 3 and Table S1 in the Supporting Information.

Physical Measurements. The infrared spectra were obtained on a Bruker Vector 22 Fourier transform infrared spectroscopy in the 4000−400 cm^{-1} regions, using KBr pellets. Elemental analyses were performed on an Elementar Vario MICRO. All of the magnetic data were recorded on a Quantum Design MPMS-XL-7 SQUID magnetometer. Variable-temperature magnetic susceptibility measurements were performed with an applied field of 100 Oe in the temperature range of 300−1.8 K. The molar magnetic susceptibilities were corrected for the diamagnetism estimated from Pascal's tables and for the sample holder by a previous calibration.

Results and Discussion

Crystal Structure of 1. X-ray crystallography reveals that complex **1** is in 3D networks. Up to date, there have been several 3D manganese−octacyanometallate bimetallic complexes reported. For the description, as further below, their structures can be roughly classified as four types by the construction: (i) A typical structure is −[W(CN)$_8$]−Mn$_4$−[W(CN)$_8$]−Mn$_4$− columnar linkages that share the nodes of Mn^{II} ions and interlock to form the 3D networks, as reported previously;[6b,i,11] (ii) The well-known [Mn$_9$M$_6$] clusters are connected by a bidentate organic ligand to the 3D cluster array;[6a,l] (iii) The square Mn$_2$W$_2$ units share the nodes of W ions leading to the 3D networks with small pores;[6b,11a,12] and (iv) [W(CN)$_8$] bridges between Mn^{II} ions with N-heterocyclic chelated ligands forming the 3D metal−organic framework.[6e,13] The structure of complex **1** is different from all the reported complexes, although it crystallizes in tetragonal system similar to those with typical structures.[6b,i,11] The asymmetrical unit of complex **1** contains an octacyanotungstate(V), 1.75 molecules of manganese(II) with 1.5 molecules of coordinating water and 0.5 molecules of formate ion and one lattice water molecule, in which most atoms are disordered in position leading to a very complicated structure. As shown in Figure 1a, octacyanotungstate takes a bicapped trigonal prismatic configuration with three disordered cyanide groups occupying four positions of C2N2 and its symmetrical sites. Thus, nine

(11) (a) Dong, W.; Sun, Y. Q.; Zhu, L. N.; Liao, D. Z.; Jiang, Z. H.; Yan., S. P.; Cheng, P. *New J. Chem.* **2003**, *27*, 1760. (b) Herrera, J. M.; Franz, P.; Podgajny, R.; Pilkington, M.; Biner, M.; Decurtins, S.; Stoeckli-Evans, H.; Neels, A.; Garde, R.; Dromzée, Y.; Julve, M.; Sieclucka, B.; Hashimoto, K.; Okhoshi, S.; Verdaguer, M. *C. R. Chim.* **2008**, *11*, 1192. (c) Ma, S. L.; Ren, S. *Russ. J. Coord. Chem.* **2009**, *35*, 766.

(12) Liu, B. L.; Xiao, H. P.; Song, Y.; You, X. Z. *Sci. China, Ser. B: Chem.* **2009**, *52*, 1801.

(13) (a) Podgajny, R.; Pinkowicz, D.; Korzeniak, T.; Nitek, W.; Rams, M.; Sieklucka, B. *Inorg. Chem.* **2007**, *46*, 10416. (b) Pinkowicz, D.; Podgajny, R.; Nitek, W.; Makarewicz, M.; Czapla, M.; Mihalik, M.; Baanda, M.; Sieklucka, B. *Inorg. Chim. Acta* **2008**, *361*, 3957. (c) Pinkowicz, D.; Podgajny, R.; Baanda, M.; Makarewicz, M.; Gawe, B.; Łasocha, W.; Sieklucka, B. *Inorg. Chem.* **2008**, *47*, 9745. (d) Yuan, M.; Gao, S.; Zhao, F.; Zhang, W.; Wang, Z. M. *Sci. China, Ser. B: Chem.* **2009**, *52*, 266.

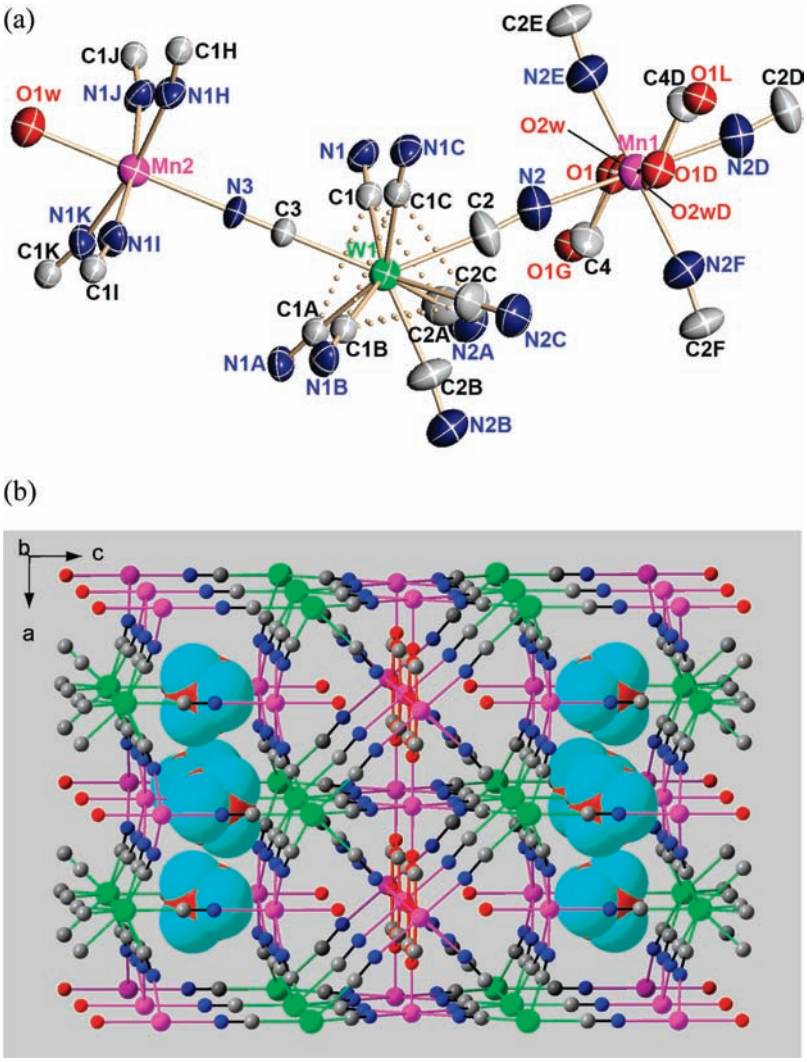

Figure 1. (a) The coordination environment around W^V and Mn^{II} ions in **1**. (b) The packing diagram of **1** shows two double-deck layers coordinating to Mn^{II} (Mn1) ions. Colors are as follows: gray, C; cyan, H; blue, N; red, O; green, W; and magenta, Mn. (symmetry code, A: $2-y, x, z$; B: $2-x, 2-y, z$; C: $y, 2-x, z$; D: $1-x, 2-y, -z$; E: $1-x, 2-y, z$; F: $x, y, -z$; G: $1-y, x, z$; H: $1.5-x, 1.5-y, 0.5-z$; I: $0.5+y, 1.5-x, 0.5-z$; J: $1.5-y, 0.5+x, 0.5-z$; K: $0.5+x, 0.5+y, 0.5-z$; L: $y, 2-x, -z$).

coordinating sites and a W^V center make up a monocapped square antiprism with C3N3 as the cap. All cyanide groups bridge from W^V to Mn^{II} ions giving rise to two coordination environments around Mn^{II} ions. The bond lengths of C−N are 1.121(8), 1.140(11), and 1.114(16) Å, while those of W−C are 2.169(7), 2.176(8), and 2.170(11) Å, respectively, comparable with the reported values.[6,11−13] Mn1 has an occupancy rate of 0.75 and accepts 0.75×4 cyanide groups by equatorial plane and 0.5×2 formate ions and 0.25×2 water molecules by the axis directions completing the six-coordinated sphere corresponding to a Mn^{II} ion. In fact, the formate ion is also a bridge between Mn1 and its asymmetrical atoms. Mn2 is coordinated by five cyanide groups of octacyanotungate(V) ions, and the residual site is occupied by a water molecule. The bond lengths of N−Mn range from 2.177(8) to 2.218(5) Å. The linkages of W−C−N−Mn are fairly linear (angles W−C≡N 173.7(9)∼180° and C≡N−Mn 170.6(6)∼180°). More important bond lengths and angles are shown in Table S1 in the Supporting Information.

In the 3D framework, C1N1 groups at first bridge between the W^V and Mn^{II} ions (Mn2) to construct a grid composed of square Mn_2W_2 units, and then C3N3 groups link the grids forming a waved double-deck structure (Figure S1 in the Supporting Information). The lattice water molecules (O3w) are filled between the grids. The linkage W1C3N3Mn2 is perpendicular to the double-deck layer, and the distance between the neighboring grids is just equal to W1C3N3Mn2, 5.480 Å. The residual three cyanide groups (C2N2) of $[W^V(CN)_8]$ coordinate to Mn1 via four disordered sites leading to the final 3D networks (Figure 1b). The short distance between the double-deck structures is 7.905 Å of W1···W1.

Crystal Structures of 2−5. Complexes **2**−**5** are isomorphous, so only the structure of complex **2** is described here. The structure of **2**−**5** is very different from that of complex **1** but similar to the typical construction reported previously.[6b,i,11] Complex **2** crystallizes in an orthorhombic system, the space group is *Ibam*. The local coordination environment of Mn^{II} ion and $[M^V(CN)_8]$ is shown in Figure 2a. In the structure, $[M^V(CN)_8]$ adopts a square antiprism geometry. Each CN group of $[W^V(CN)_8]$ coordinates to eight Mn^{II} ions forming a $-[W(CN)_8]-Mn_4-[W(CN)_8]-Mn_4-$ columnar chain. All chains share Mn^{II} ions as the nodes and interlock with each other to form the 3D

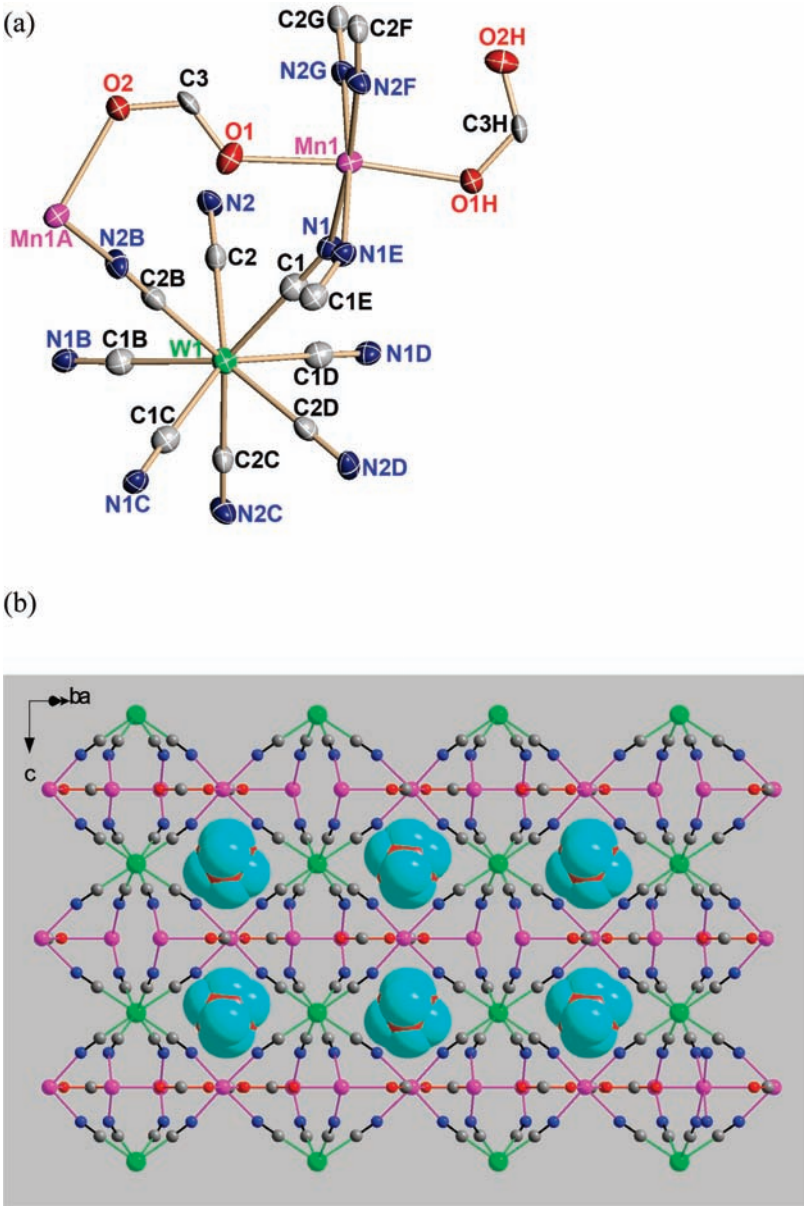

Figure 2. (a) The local coordination environment around W^V and Mn^{II} ions in **2**. (b) The packing diagram of **2**. Colors are as follows: gray, C; cyan, H; blue, N; red, O; green, W; and magenta, Mn. (symmetry code, A: $x-1.5, -y-0.5, z$; B: $-x, y, 0.5-z$; C: $-x, 1-y, z$; D: $x, 1-y, 0.5-z$; E: $x, y, -z$; F: $0.5-x, 0.5-y, z-0.5$; G: $0.5-x, 0.5-y, 0.5-z$; H: $x-0.5, -y-0.5, z$).

structure as shown in Figure 2b. The Mn^{II} ion is located in the center of an octahedron. Four cyanides of different $[W^V(CN)_8]$ groups are ligated to a Mn^{II} ion in the equatorial plane, and two formic anions occupy the axis positions. Simultaneously, the formic anion bridges between two Mn^{II} ions in syn−anti coordination conformation. W1−C2B−N2B−Mn1A linkage is almost linear (angles W−C≡N 177.7(4) and C≡N−Mn 168.4(4)°), but W1−C1−N1−Mn1 exhibits a larger bend extent (angles W−C≡N 178.7(4) and C≡N−Mn 154.1(4)°). All bond lengths and angles in **2**−**5** are slightly different from those of the reference complexes with chloride or acetate ions[6b,i] but very close to those without additional ligands,[11a,b] because the latter have two kinds of CN bridges. The corresponding bond lengths and angles of **2**−**5** and the shortest distance between Mn^{II} and W^V ions are listed in Table 3 for comparison. Four complexes of **2**−**5** all contain solvent molecules in the lattice. However, the very little change of solvent in the synthesis leads to the different guest molecules, water molecules in **2** and **3** and methanol molecules in **4** and **5**.

Magnetic Properties of 1. Variable-temperature magnetic measurements were performed on polycrystalline samples of complex **1** in the range of 1.8−300 K in 100 Oe, as shown in Figure 3 and Figure S3 in the Supporting Information. The $\chi_M T$ value at room temperature is 7.04 cm^3 K mol^{-1}, which is less than the spin-only value of 8.03 cm^3 K mol^{-1} for the $W^V Mn^{II}_{1.75}$ system ($S_{W(V)} = 1/2$, $S_{Mn(II)} = 5/2$, assuming $g_{W(V)} = g_{Mn(II)} = 2.0$). As the temperature decreases, the $\chi_M T$ value gradually increases until 60 K. When the temperature is below 60 K, $\chi_M T$ abruptly increases to a maximum of 2580.8 cm^3 K mol^{-1} at 52 K and then quickly drops to 105.3 cm^3 K mol^{-1} at 1.8 K. The abrupt increase of 300 times in $\chi_M T$ indicates the formation of magnetic domains due to the long-range ordering in complex **1**. This can be supported by the low-field variable-temperature magnetic measurements.

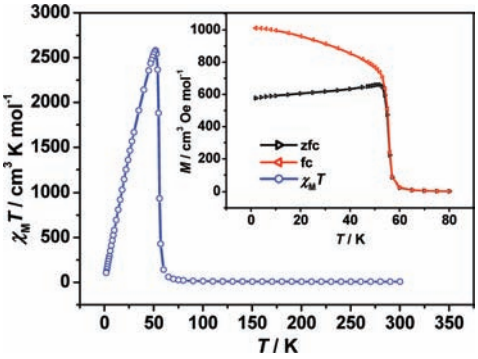

Figure 3. The temperature dependence of magnetic properties for complex **1** in the form of $\chi_M T$. The inset is ZFC and FC magnetization in an applied field of 10 Oe.

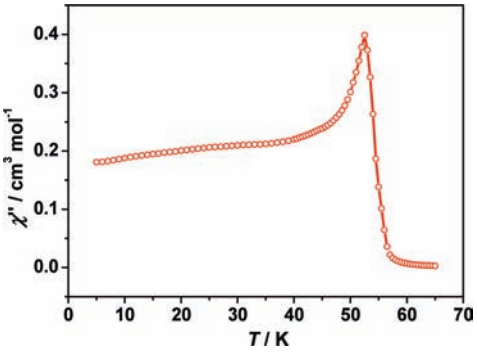

Figure 4. The out-of-phase variable-temperature AC magnetic susceptibility for complex **1** measured in $H_{dc} = 0, f = 10$ Hz, and $H_{ac} = 4$ Oe.

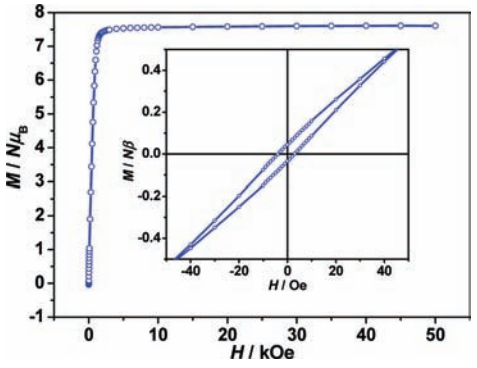

Figure 5. The field dependence of magnetization for complex **1** at 2 K.

The magnetization after zero-field cool (ZFC) and subsequent field cool (FC) in 10 Oe reveals nonreversibility and bifurcation as shown in the inset in Figure 3, indicating the occurrence of magnetic ordering below ~53 K. Similarly, both of out-of- and in-phase AC magnetic susceptibilities (Figure 4 and Figure S4 in the Supporting Information) show the peaks at around 53 K, further indicating the presence of the magnetic phase transition at this temperature. At 2 K the variable-field magnetization was measured. As shown in Figure 5, complex **1** is very easily magnetized and reaches saturation above 2 kOe. In 5 T, the saturation value of magnetization is 7.61 $N\mu_B$, which is in good agreement with the theoretical value of 7.75 $N\mu_B$ ($1.75 \times 5/2 \times 2 - 1 \times 1/2 \times 2$) for antiferromagnetic coupling between W^V and Mn^{II} ions, indicating that complex **1** is a ferrimagnet. A very small loop is observed showing a coercive field of 4 Oe at 2 K. This implies that

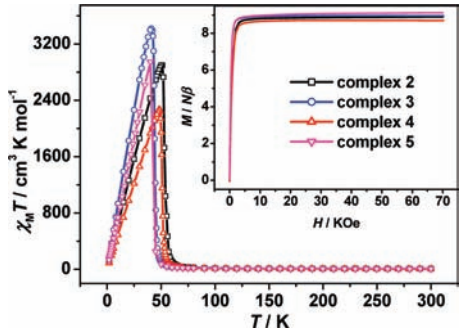

Figure 6. The temperature dependence of magnetic properties for complexes **2**−**5** in the form of $\chi_M T$. The inset corresponds to their variable-field magnetization at 1.8 K.

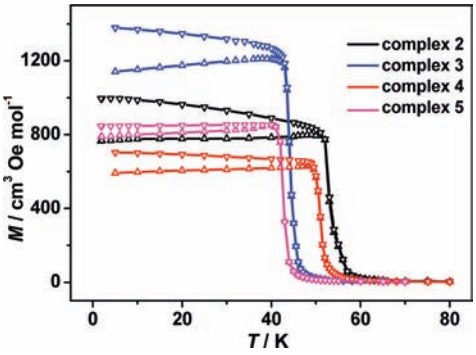

Figure 7. The ZFC and FC magnetization of complexes **2**−**5** in an applied field of 10 Oe.

complex **1** is a soft magnet. From the curve of the variable-temperature magnetic properties, the increase of $\chi_M T$ as system cooling cannot be ascribed to ferromagnetic coupling between W^V and Mn^{II} ions in complex **1**. However, this behavior is universally observed in octacyanometallate-based complexes. It is believed that the large diffusion of the 4d and 5d orbitals will lead to coupling interaction in a wide range of temperature,[3a,d,j,6a,b] thus resulting in the antiferromagnetic coupling between W^V and Mn^{II} ions and the minimum $\chi_M T$ at higher temperature than room temperature.

Magnetic Properties of 2−5. The magnetic measurements of complexes **2**−**5** were also performed on polycrystalline samples and with the same test conditions as complex **1**. Owing to the very similar structure, the magnetic properties of **2**−**5** are comparable. So hererin, we only describe the properties of complex **2** in detail. As shown in Figure 6 and Figure S5 in the Supporting Information, complex **2** shows the similar variable-temperature magnetic properties to complex **1**. As the system cools down, the $\chi_M T$ value gradually increases from 8.84 cm^3 K mol^{-1} at room temperature to 90.5 cm^3 K mol^{-1} at 61 K and then abruptly increases going through a maximum of 2898.2 cm^3 K mol^{-1} at 51 K, finally sharply decreasing to 115.7 cm^3 K mol^{-1} at 1.8 K. The ZFC and FC curves are nonreversible, and a bifurcation occurs at ~52 K (Figure 7). Also, the peaks are observed around 52 K in both out-of- and in-phase AC magnetic measurements (Figure 8 and Figure S6 in the Supporting Information). All these facts suggest the formation of 3D magnetic ordering below 52 K in complex **2**. The variable-field measurements at 1.8 K show that the magnetic

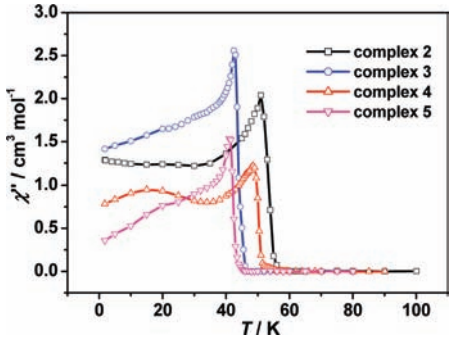

Figure 8. The out-of-phase variable-temperature AC magnetic susceptibility for complexes **2**−**5** measured in $H_{dc} = 0$, $f = 10$ Hz, and $H_{ac} = 1$ Oe.

Table 4. Some Magnetic Data of Complexes **2**−**5**

	$\chi_M T$ (cm^3 K mol^{-1})					
complex	*RT*	max.	1.8 K	T_c (K)	saturation field (kOe)	saturation value at 7 T ($N\mu_B$)
2	8.84	2898.2	115.7	52	∼4	8.90
3	8.94	3425.7	169.5	42	∼3	8.97
4	7.64	2269.6	89.1	49	∼4	8.72
5	8.99	2949.9	132.9	41	∼3	9.13

properties of complex **2** are saturated above 4 kOe, and the saturation moment is 8.90 $N\mu_B$, indicating that complex **2** is also a ferrimagnet (theoretical value equals to $2 \times 5/2 \times 2 - 1 \times 1/2 \times 2 = 9$ $N\mu_B$). In the M−H curve, no hysteresis loop is observed, so complex **2** is a soft magnet.

Generally, all complexes **2**−**5** are the soft ferrimagnets. According to the theoretical analysis reported previously in literature,[6b] cyano bridges provide three super-exchange pathways between Mn^{II} and M^{V} (M = Mo or W) in a square antiprismatic environment. The sole half-filled d_{z^2} orbital of M^{V} ion and the d_{xy} orbital of Mn^{II} ion produce a π pathway, while the d_{z^2} and $d_{x^2-y^2}$ orbitals of the Mn^{II} ion lead to two σ pathways. All these pathways mediate the antiferromagnetic coupling between Mn^{II} and M^{V}, but the π component provides the main magnetic coupling interaction due to the low energy. Complexes **2**−**5** show the same framework in 3D construction with square antiprismatic $[M^{V}(CN)_8]$ bridging between the Mn^{II} ions, so all of them behave as ferrimagnet. However, the different octacyanometallate groups and the guest molecules in the lattice give rise to variation in magnetic properties. For comparison, some important magnetic data are listed in Table 4. When the guest solvent is the same, the magnetic ordering temperature T_c of a tungstate-based complex is about 10 K higher than that of a molybdate-based complex. This behavior can be well ascribed to the heavy-atom effect of metal ions,[3a,d,j,6a,b] namely, 5d orbitals with radial distribution far from the nucleus of tungsten are more advantageous to overlap with the magnetic orbitals of neighboring manganese ions than those of 4d orbitals of molybdenum. Therefore, the coupling interaction ($J_{M_AM_B}$) between W^{V} and Mn^{II} ions is stronger than that between Mo^{V} and Mn^{II} ions. According to the molecule field theory described in eq 1,[14] the interaction will further increase the magnetic phase transition temperature of complexes **2** and **4** comparing with complexes **3** and **5**, respectively.

$$T_C = \frac{2\sqrt{Z_{M_A}Z_{M_B}}|J_{M_AM_B}|\sqrt{S_{M_A}(S_{M_A}+1)S_{M_B}(S_{M_B}+1)}}{3k} \quad (1)$$

where Z_M is the number of the nearest neighbors bridged to M, k is Boltzmann constant (0.69372 cm^{-1} K^{-1}), and $J_{M_AM_B}$ is the exchange coupling constant between the M_A and M_B ions.

The second phenomenon is that the magnets with water as the guest solvent show a slightly higher critical temperature than those with the methanol solvent. From the crystal structures (Tables 2 and 3), we can find that the *a* and *b* axes of the unit cell in complexes **4** and **5** are elongated, so the corresponding unit cell is larger than those of complexes **2** and **3**. It can be attributed to the larger size of methanol molecule. The bond lengths of M−CN of complexes **4** and **5** are remarkably longer than those of **2** and **3**, as shown in Table 3. For the same coupling pathway, the longer distance between metal ions will certainly reduce the overlap between orbitals, further weakening their coupling interaction $J_{M_AM_B}$. Thus, the magnetic critical temperatures of **4** and **5** are slightly lower than those of **2** and **3** (eq 1).

The third phenomenon is that complexes **2**−**5** show a higher critical temperature than those with same type of structure reported previously.[6b,i] In reference complexes, the accessional ligands are chloride, water or anti−anti acetate, which mediates the antiferromagnetic coupling (mediated by acetate) or no coupling interaction (terminal ligands of chloride or water) between Mn^{II} ions. Based on the magnetic structure of reference complexes, antiferromagnetic coupling between Mn^{II} ions weakens the coupling $J_{M_AM_B}$ between M^{V} and Mn^{II} ions due to the competition between two sets of coupling interactions. However, a syn−anti carboxylate bridge of formate mediating ferromagnetic coupling between Mn^{II} ions[15] in complexes **2**−**5** may provide a synergy effect to strengthen the coupling between M^{V} and Mn^{II} ions, further increasing their magnetic phase transition temperature.

In summary, five manganese(II)−octacyanometallate-(V) bimetallic complexes **1**−**5** were synthesized in acidic media. By adjusting starting octacyanometallates $A_3[M(CN)_8]\cdot nH_2O$ (A = Na, Cs, and $(C_4H_9)_3NH$; M = W and Mo; and n = 2 or 4) and manganese salts ($Mn(CH_3COO)_2\cdot 4H_2O$, $Mn(ClO_4)_2\cdot 6H_2O$, and $MnCl_2\cdot 4H_2O$), different products can be obtained in the aqueous or methanol solution of formic acid. Complex **1** shows a rare three-dimensional (3D) structure with an alternative $-(W_2Mn_2)_n-(Mn)_m-$ linkage of double-deck layers and Mn^{II} ions, while complexes **2**−**5** have the typical construction similar to the reference complexes reported previously.[6b,i,11] Magnetic investigation shows that all complexes **1**−**5** are ferrimagnets below 53, 52, 42, 49, and 41 K, respectively. The heavy-atom effect on magnetic properties is clearly shown in the contrast group between **2** and **3** or **4** and **5**. The perturbation of solvent in the lattice leads to the difference magnetic

(14) Ohkoshi, S.; Iyoda, T.; Fujishima, A.; Hashimoto, K. *Phys. Rev. B: Solid State* **1997**-II, *56*, 11642.

(15) Konar, S.; Mukherjee, P. S.; Drew, M. G. B.; Ribas, J.; Chaudhuri, N. R. *Inorg. Chem.* **2003**, *42*, 2545 and references therein.

properties. Formate groups mediate ferromagnetic coupling interaction between Mn^{II} ions, resulting in a higher critical temperature in **2**−**5** than in reference complexes.

Acknowledgment. The authors thank the Major State Basic Research Development Program (2007CB925102 and 2006CB806104) and the National Natural Science Foundation of China (20721002, 20631030 and 20771057) for the financial support to this work.

Supporting Information Available: X-ray crystallographic data for complex **1**−**5** in CIF format and selected bond lengths and angles for complex **1** in Table S1. Additional magnetic analysis in Figures S3−S6. This material is available free of charge via the Internet at http://pubs.acs.org.